

Discrete-time Robust Fault Detection Observer Design: a Simulated Annealing Approach

Xuewu Dai* Yiqun Zou* Tim Breikin* William Heath*

* *Control Systems Centre, The University of Manchester,
Manchester UK, M60 1QD.*

Abstract: The RFDO (Robust Fault Detection Observer) has been an important branch of fault detection during the last two decades. However, most of current research focuses on the continuous-time domain and requires relatively more computation. In this paper, with the aid of the well-established eigenstructure assignment, a frequency weighted robustness index is proposed for reducing the computation costs and a left-eigenvector assignment method is presented for discrete RFDO design. A simulated annealing algorithm is then applied to optimise such an observer. As illustrated in the simulation results, a better performance has been obtained. Compared to the previous studies, simulated annealing gives the similar results as genetic algorithm, but requires a bit of less computation.

1. INTRODUCTION

The design of RFDO (Robust Fault Detection Observer) has received much attention during the last two decades. (see for instance El-Ghatwary et al. [2006], Frank and Ding [1997], Chen and Patton [1999]). The basic idea is to eliminate the effects of disturbances on the residuals. Because full disturbance decoupling requires strict conditions, in recent years, more research has been done on approximate decoupling, where disturbances are attenuated as much as possible by using optimisation techniques.

Eigenstructure assignment has been successfully applied to observer design, where the observer gain matrix and transfer function matrices (TFMs) are parameterised by a set of closed-loop poles and a set of free parameters (Patton and Chen [2000], Liu and Patton [1998]). Furthermore, it is well known that the solution of eigenstructure assignment is not unique and it is possible for designing an observer to meet additional robustness and sensitivity criteria. As a consequence, the RFDO design turns into an optimisation problems (Chen and Patton [1999], Patton and Chen [2000], Liu and Patton [1998]). With the aid of the well-established H_∞ control theories, some researchers built robust observer by minimising H_∞ (Wang et al. [2007a]), H_2 , H_- (Hou and Patton [1996], Jaimoukha et al. [2006]) indices.

However, the H_∞ index requires relative more computation, because an integral or gridding over the whole frequency range is required. Moreover, the H_∞ observer is designed for the worst case by minimising the peak of TFMs at some frequency w_p . Note that w_p is determined by TFMs, not by disturbances. As it only gives the basic guarantee of the performance at the worst-case, the H_∞

optimal observer may be too conservative in some practical applications. In order to achieve a better disturbance attenuation performance and reduce the complexity, more research is needed on discrete robust fault detection observer (DRFDO) design in frequency domain.

On the optimisation of the performance indices, many algorithms, such as gradient based optimisation (Liu and Patton [1998]), LMI (Wang et al. [2007b]) have been proposed. Since at the first time its idea was adopted in Metropolis-Hastings algorithm (Teller and Teller [1953]) in 1953 and described by (Kirkpatrick et al. [1983]), simulated annealing is explicitly examined in terms of optimisation (T.W.Manikas and J.T.Cain [1996]). And its results are very satisfactory for avoiding the gradient search trapped in the vicinity of local minima because the information of cost function does not need to be known beforehand. In the scope of this paper, we have novelly exploited the simulated annealing approach in discrete fault detection observer design.

In this paper, the problem of DRFDO is first formulated in section II. Section III presents the parameterisation of observer gain matrix K by eigenstructure decomposition, and a new frequency-dependent performance index is proposed for reducing the computation costs. At the optimisation step, a simulated annealing algorithm is used in section IV. Section V shows the simulation results. The main contribution of this paper could be the reduction of computation complexity and further improvement on disturbance attenuation by integrating disturbance frequency information into the performance index.

2. PROBLEM FORMULATION

Consider a general case of noise/disturbance corrupted system in a discrete-time state space form:

$$\begin{cases} x(k+1) = Ax(k) + Bu(k) + B_f f(k) + B_d d(k) \\ y(k) = Cx(k) + Du(k) + D_f f(k) + D_d d(k) \end{cases} \quad (1)$$

* This work was partially supported by the EPSRC grant EP/C015185/1. The authors email addresses are: daixuewu@hotmail.com, yiqunzou@gmail.com, t.breikin@manchester.ac.uk and William.Heath@manchester.ac.uk, respectively.

$$(zI - A + KC)^{-1} = \frac{r_1 l_1^T}{z - \lambda_1} + \frac{r_2 l_2^T}{z - \lambda_2} + \dots + \frac{r_n l_n^T}{z - \lambda_n} \quad (12)$$

Substituting (12) into (5) gives the parametric expressions of $G_d(z)$ and $G_f(z)$. Then rewriting it into matrix form gives (8), (9). Proved.

It is worthy noting that, under the assumption of distinct closed-loop poles from open-loop poles and the constraint of self-conjugated poles, the parameters $\{\lambda_i\}$, $\{q_i\}$ can arbitrarily be chosen from the fields \mathbb{C} of complex numbers and from the vector spaces \mathbb{C}^p , respectively.

It can be seen from this lemma that all the vectors l_i , r_i and matrix L , R depend on the choice of λ_i and q_i^T ($i = 1, 2, \dots, n$). The explicit parametric expression of TFMs $G_d(z)$ and $G_f(z)$ makes it easy to use the simulated annealing algorithm to find the optimal gain matrix K , as the stability constraints are met by simply setting the boundaries of eigenvalues λ_i .

3.2 Performance Index Evaluation

If the disturbance TFM $G_d(z)$ is designed to satisfy $G_d(z) = 0$, it leads to perfect de-coupling which means the disturbance is totally de-coupled from the residual $r(k)$. Such a full disturbance de-coupling has been proposed by using UIOs, orthogonal eigenstructure assignment, and some frequency domain design technique.

However, $G_d(z) = 0$ requires stronger conditions which are not always met. Therefore, an optimal (or approximate) de-coupling is proposed by minimizing a performance index containing the robustness to disturbances $d(z)$ and maximising a performance index of the sensitivity to faults $f(z)$. One of such performance indices defined in the frequency domain can be written as:

$$J_{\infty/\infty} = \frac{\|G_d(z)\|_{\infty}}{\|G_f(z)\|_{\infty}} \quad (13)$$

where a H_{∞} -norm of a TFM is used. Although H_{∞} -norms are widely adopted, different matrix norms (such as H_2 -norm, H_{∞} -norm, Frobenius norm) are also suggested and have different characteristics (Chen and Patton [1999]). In the widely adopted H_{∞} -norms, the robustness and sensitivity are optimised at the worst-case. There are two main drawbacks in H_{∞} -norm based performance index. One is the computation complexity, as computing H_{∞} -norm requires gridding over the whole frequency range $[0, \pi]$ and finding the largest singular value of a matrix. The computation burden is very high during the optimisation procedure. It is particularly true for stochastic optimisation algorithm which needs a lot of evaluations of objective function. Another drawback is that the worst case does not represent all possible disturbances. The H_{∞} -norm based observer is only optimal at the worst-case, not in all the possible situations. It can be imagined that, if the performance index is optimised over the disturbance frequency, rather than the worst case, such an observer is more robust to the disturbance.

Robustness Performance Index Based on the observation above, a performance index is proposed here by replacing the common H_{∞} -norm with the TFMs norm evaluated at disturbance frequencies. If the frequency band of the

disturbance is available, no matter it is bounded or not, the residual can be designed maximally robust to the disturbances by optimising the performance index at the frequency band w_d .

$$\min J_1 = \|G_d(z)\|_{z=e^{jw_d}} \quad (14)$$

where w_d denotes the main frequency of the disturbance. Substituting (8) into J_1 gives

$$\min J_1 = \|D_d + C [R\Psi(e^{jw_d})L] (B_d - L^{-1}QD_d)\| \quad (15)$$

Since the disturbance is still unknown, the key issue in evaluating the performance index (15) is to estimate the disturbance frequency w_d . Fortunately, the disturbance frequency can be estimated from the residual spectrum analysis, according to the property that the input frequency has not changes, only the amplitude and phase angle of the sinusoid has been changed by linear systems.

In this new performance index (15), the disturbance frequency information is incorporated, and the resulting observer is optimal for attenuating such a disturbance. In most cases, such an observer should have better disturbance attenuation performance than the observer designed by optimising H_{∞} -norm.

Sensitivity Performance Index From a frequency domain viewpoint, most faults have some specific characteristics. In most applications, for example, an incipient fault comprises mainly low frequency components. As seen in (Chen and Patton [1999]), for abrupt faults, high frequency contents only exist at the time instant when faults begin, and it is almost constant components thereafter. Considering this, a strong fault detectability condition of the residual r to the fault f : $|G_f(0)| \neq 0$ is proposed. Therefore, in order to reflect the shape variations of the fault signal, the most important factor in fault detection for DRFDO is the steady state gain matrix $G_f(z)|_{z=1}$. Hence the $G_f(z)|_{z=1}$ index should be maximised for increasing fault detectability. In this paper, the sensitive performance index is then defined as

$$\max J_2 = \|G_f(z)\|_{z=1} \quad (16)$$

Substituting (9) into J_2 gives

$$\max J_2 = \|D_f + C [R\Psi(1)L] (B_f - L^{-1}QD_f)\| \quad (17)$$

Remark: There is some equivalence between the new sensitive index (17) and the commonly used $\|G_f(z)\|_{\infty}$. As most plant systems in practice are low pass systems in terms of frequency response, the peak value of the magnitude response of such a transfer function is at zero frequency. Thus, the H_{∞} -norm of $\|G_f(z)\|_{\infty}$ is equal to $\|G_f(z)\|_{z=1}$. The benefit is that the computation of $\|G_f(z)\|_{z=1}$ is less than that of H_{∞} -norm.

It should be noted that, the proposed performance indices (15), (17) are frequency dependent. The disturbance frequency information and the frequency characteristics of faults are integrated into the performance indices, which is the significant difference from H_{∞} based indices.

4. OBSERVER OPTIMISATION VIA SIMULATED ANNEALING

As seen in the preceding section, there are two objectives to be optimised. In order to achieve an approximated

global optimal solution, this section concerns with the application of simulated annealing optimisation algorithm. The general idea of simulated annealing is to decide whether to replace the current solution with the trial solution selected randomly in the nearby neighborhood after each iteration based on the difference between the cost function values of two solutions and cooling temperature T , where T decreases gradually in the annealing period. When T is moderately large, there is a relatively high probability that some "uphill" movements will be approved throughout the process. Once T asymptotically approaches zero, only "downhill" replacement will occur.

Before specifying the explicit procedure of the optimisation algorithm, we first define some useful expressions:

(1) **Vector reshaped-representation of objective matrix.** The simulated annealing is a numerical optimisation algorithm which concerns only in the numerical values of the parameter vector. For parameters $Z \in \mathbb{R}^n$ and $Q \in \mathbb{R}^{n \times p}$, the reshaped-representation of the parameter matrices can be expressed as a vector:

$$\theta = [q_1^T, \dots, q_n^T, \lambda_1, \dots, \lambda_n,] \quad (18)$$

where the total number of parameters in θ is $n + n \times p$.

(2) **Cost Function.** Evaluate the cost function for the parameter vector θ ,

$$C = \frac{1}{J}$$

and

$$J = \frac{\|G_d(z, \theta)\|_{z=1}}{\|G_f(z, \theta)\|_{z=e^{j\omega_d}}}$$

where $\|G_d(z, \theta)\|_{z=1}$, $\|G_f(z, \theta)\|_{z=e^{j\omega_d}}$ denote the robustness and sensitivity indices (15) and (17), respectively.

Now we are about to summarize the following five steps usually involved in simulated annealing optimisation:

Step 1: Initialization Algorithms normally should be initialized before operation. At this stage, we carefully choose the parameter vector θ and the starting cooling temperature T_o , etc. The only attention needs to be paid on the absolute value of system poles which should be less than one in order to maintain the system stability.

Step 2: Cooling Scheme Selection To accelerate the algorithm convergence speed, we select the fast annealing scheme H.Szu and R.Hartley [1987]:

$$T_k = \frac{T_o}{1+k} \quad (19)$$

where k indicates the iteration time.

Step 3: Trial Solution Calculation In this step, a trial solution is picked up randomly in the nearby neighborhood of θ_k , where θ_k denotes the values of parameters at k -th iteration. A scalar constant λ is set to adjust the step size of the change between θ_{tri} and θ . In MATLAB, the numerical relationship is described as below:

$$\theta_{tri} = \theta_k + \lambda \text{randn}(\text{dim}(\theta), 1) \quad (20)$$

where $\text{dim}(\theta)$ denotes the dimension of θ . $\text{randn}(\text{dim}(\theta))$ returns a vector consists of $\text{dim}(\theta)$ random numbers.

Step 4: Determination of Substitution Based on θ_{tri} and θ_k , the cost function value of each could be derived as C_{tri} and C_k respectively. Then we compare

$$C_{dif} = C_{tri} - C_k \quad (21)$$

with T . If $C_{dif} < T$ while other constraint conditions are met, θ will be substituted by θ_{tri} (P.Salamon and Frost [2002]). Otherwise the same θ is retained in next iteration.

$$\begin{cases} \theta_{k+1} = \theta_{tri} & \text{if } C_{dif} < T \\ \theta_{k+1} = \theta_k & \text{otherwise} \end{cases} \quad (22)$$

Step 5: Termination Rule Terminate the algorithm if the stopping criterion is achieved or a maximum iteration time is reached, otherwise go back to Step 2 to continue the programme. The stop criterion is

$$\frac{|C_k - C_{k-M}|}{C_k} < \varepsilon \quad (23)$$

where C_k and C_{k-M} both are cost function values in different iteration times between which C_k is after C_{k-M} M times. And ε is a very small positive constant. Both M and ε are defined empirically in priori.

5. SIMULATION AND RESULTS

To illustrate the proposed observer optimisation approach, this section concerns with robust fault detection of a dynamic system. Both abrupt and incipient actuator faults are considered in this simulation. The parameter matrices of the dynamic system are given as follows:

$$A = \begin{bmatrix} 0.9769 & 0.0038 \\ 0.0936 & 0.9225 \end{bmatrix}, \quad B = \begin{bmatrix} 2.1521 \\ 3.8186 \end{bmatrix}, \quad (24)$$

$$C = \begin{bmatrix} 1 & 0 \\ 0 & 1 \end{bmatrix}, \quad D = \begin{bmatrix} 0 \\ 0 \end{bmatrix}$$

and the sampling rate is 40Hz. The disturbance model and fault model are

$$B_d = \begin{bmatrix} 0.1510 & 0.0406 \\ 0.0500 & 0.0528 \end{bmatrix}, \quad B_f = B, \quad (25)$$

$$D_d = \begin{bmatrix} 0 & 0 \\ 0 & 0 \end{bmatrix}, \quad D_f = \begin{bmatrix} 0 \\ 0 \end{bmatrix}$$

where the fault matrix $B_f = B$ for actuator fault, $D_f = 0$ indicates fault-free output sensors. The external disturbances injected to the systems are

$$\mathbf{d}(k) := \begin{cases} d_1(k) = 0.1\sin(2k) + 0.1\cos(2.1k + \frac{\pi}{4}) \\ d_2(k) = 0.05\sin(2.1k) \end{cases} \quad (26)$$

where the main frequency components are at frequencies of 2 rad/sec and 2.1 rad/sec. Since these two frequencies are very close to each other and the magnitude response of a dynamic system is generally a continuous smooth function, it does not matter much to set the disturbance frequency w_d as 2.0 or 2.1. In this simulation, let $w_d = 2.1$ for the evaluation of the robustness index (15).

For simplification, the desired poles are real and the allowed region is $(-0.95, 0.95)$.

In the implementation of simulated annealing optimisation, the starting cooling temperature $T_o = 1$ for a relatively large initial uphill movement. The allowed maximum step size $\lambda = 0.1$. The stop condition are $\varepsilon = 1 \times 10^{-6}$ and $M = 500$ for guaranteeing the final convergence. The simulated annealing procedure ends when the change ratio between 500 iterations is smaller than ε .

The optimisation progress of this simulated annealing algorithm is shown in Fig. 2. The final solution is $\theta_b =$

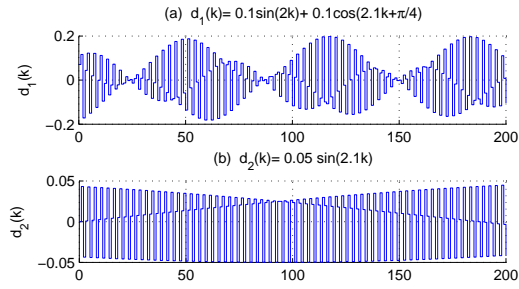


Fig. 1. Disturbances injected to the system.

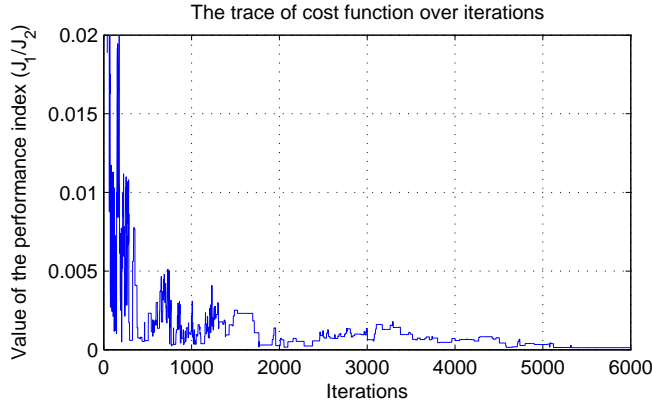


Fig. 2. Trace of the cost function values over iterations in the simulated annealing optimisation. It involves 6000 search iterations and one cost function evaluation in each iteration. In total, the number of objective function evaluation in this simulated annealing optimisation is 6000.

$[4.2415 \ 2.0871 \ 3.5304 \ 0.5367 \ 0.8914 \ 0.9081]^T$. In this implementation, the search process stops after the maximum number of iterations (6000 iterations) is reached with the resulting gain matrix

$$K_{sa} = \begin{bmatrix} -8.7312 & 12.6588 \\ -6.0374 & 8.8311 \end{bmatrix} \quad (27)$$

which gives the performance index $J = 8.3565 \times 10^{-5}$ and optimal poles (0.9081 0.8914).

For comparison, two other methods are also used to compute the gain matrix. The resulting matrices, performance indices and poles are shown in Table 1, where K_{opt} is

Table 1. Comparison of Different Methods

| | Gain Matrix | J_1/J_2 | poles | Costs* |
|-------------|--|-----------------------|--|--------|
| K_{opt} | $\begin{pmatrix} 3.3769 & -11.058 \\ 0.9516 & -2.8394 \end{pmatrix}$ | 5.58×10^{-4} | $\begin{pmatrix} 0.6519 \\ 0.71 \end{pmatrix}$ | 5760 |
| K_{place} | $\begin{pmatrix} 0.1320 & 0.0038 \\ 0.0936 & 0.0029 \end{pmatrix}$ | / | $\begin{pmatrix} 0.8914 \\ 0.9081 \end{pmatrix}$ | / |
| K_{ga} | $\begin{pmatrix} -8.731 & 12.659 \\ -6.037 & 8.8311 \end{pmatrix}$ | 5.55×10^{-5} | $\begin{pmatrix} 0.8449 \\ 0.9196 \end{pmatrix}$ | 8000 |

note:

* The costs of the optimisation algorithm is measured by how many objective function evaluations are involved in the optimisation process.

optimised by using $fmincon()$ provided by MATLAB Optimisation Toolbox. K_{place} is computed by using $place$ command in MATLAB Control Toolbox. K_{ga} is optimised by the Genetic Algorithm and Direct Search Toolbox. For

a fair comparison, the K_{place} is set with the identical eigenvalues as K_{sa} . From the Table 1, it can be seen that, the genetic algorithm gives a bit smaller value of performance index at higher computation costs (the cost of the genetic algorithm is 2000 more than that of the simulated annealing). Since the difference between these two index values is ignorable (at the order of 10^{-5}), simulated annealing optimisation achieves a similar performance paid by a relatively lower computation cost.

5.1 Residuals of abrupt Faults

In this trial, the fault is simulated by the following function:

$$f(t) = \begin{cases} 0 & t < 5 \\ 0.001 & t \geq 5 \end{cases} \quad (28)$$

The residual norms $|r(k)|_{sa}$, $|r(k)|_{ga}$, $|r(k)|_{opt}$ and $|r(k)|_{place}$ corresponding to this abrupt fault are shown in Fig. 3, respectively. It can be seen that there is a relatively large overshoot in both $|r(k)|_{sa}$ and $|r(k)|_{ga}$ at the beginning due to the dynamic process of the observer.

The observer K_{place} fails to detect such an abrupt fault, as there is no apparent change in its residual after fault happening. K_{opt} gives a slight step increase in its residual soon after the fault occurring, but the magnitude of the change is too small (less than 0.5) which may leads to missed alarms. However, the residual norm of K_{sa} presents an obvious step increase right after the fault happens. At 6 second, $|r(k)|_{sa}$ achieves 4 which is about 8 times of the fault-free residual norm. A similar result is given by K_{ga} . The residual variation of $|r(k)|_{ga}$ is smaller than that of $|r(k)|_{sa}$. In $|r(k)|_{sa}$ and $|r(k)|_{ga}$, there are enough margins to ensure the detection of such an abrupt actuator fault.

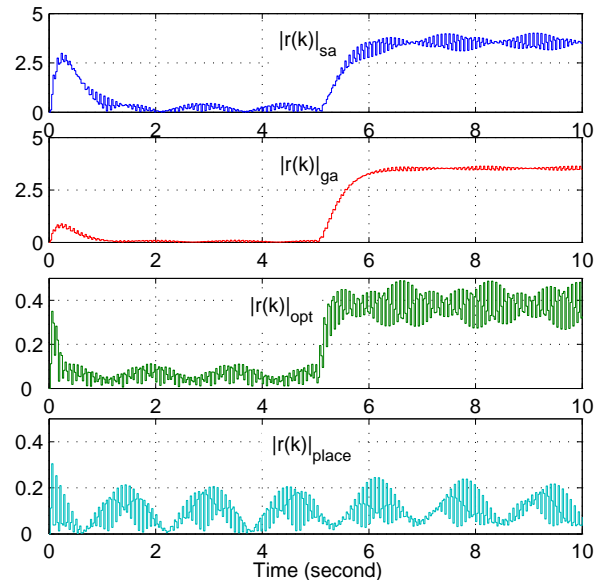


Fig. 3. Residual norms of K_{sa} , K_{ga} , K_{opt} and K_{place} , corresponding to the abrupt fault (28)

5.2 Residuals of Incipient Faults

The ability of the proposed DRFDO to detect drifting faults is also evaluated here. Such incipient faults are

extremely difficult to be detected immediately from a simple visual inspection of the output signals. In this trial, an incipient actuator fault is simulated by

$$f(t) = \begin{cases} 0 & t < 5 \\ 0.001(t-5) & 5 \leq t \leq 8 \\ 0.003 & 8 \leq t \leq 9 \\ 0.003 - 0.002(t-9) & 9 \leq t \leq 10 \end{cases} \quad (29)$$

as shown in Fig. 4. The corresponding residuals are shown in Figure 5. Both observer K_{sa} and K_{ga} give the similar results where the residuals are able to follow the changes of the fault. In $|r(k)|_{opt}$ and $|r(k)|_{place}$, although some slight up trends can be noticed, but it is hard to distinguish faulty residuals from the fault-free residuals. Similar to the abrupt fault detection, $|r(k)|_{sa}$ shows a similar abilities as the observer optimised by genetic algorithms and the improvement on detecting incipient faults is reached. Particularly, the earlier detection of incipient faults has a

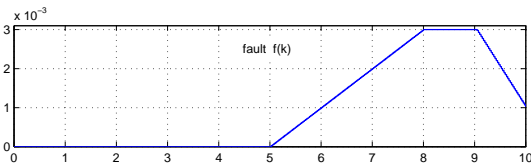


Fig. 4. The fault signal of Eq. (29).

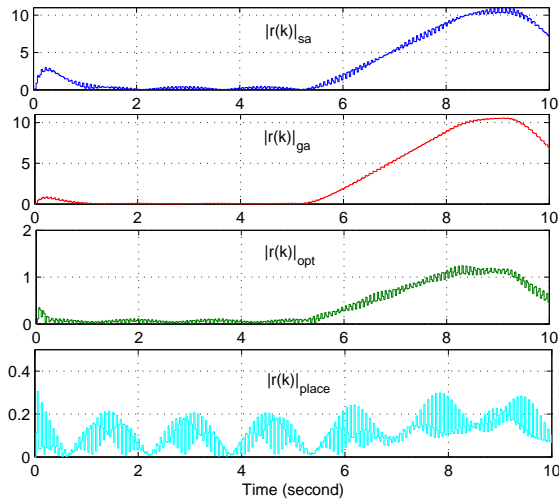


Fig. 5. Residual norms of K_{ga} (blue), K_{opt} (read), K_{place} (green), corresponding to the incipient fault (slope=0.00001)

lot of benefits for reliable operation and reducing maintenance costs.

6. CONCLUSION

This paper demonstrates a discrete observer design method through eigenstructure assignment. The only assumption on the external disturbance is band-limited frequency distribution. Then a frequency dependent robustness/sensitivity performance index is formed and parameterised by left eigenvector assignment. Finally, the simulated annealing algorithm is used to find the optimal solution to the observer gain matrix K .

As shown in the simulation results, such an observer optimised by annealing algorithm achieves a similar performance as genetic optimisation. But the computation costs

of simulated annealing algorithm is lower than that of genetic algorithms. Although this is designed for attenuating external disturbances, the principles used here are also applicable to the problem of model uncertainty. The difficulty, however, lies at that the disturbance caused by model uncertainty is also related with the input signals which may not be band-limited.

REFERENCES

- Jie Chen and R.J. Patton. *Robust Model-Based Fault Diagnosis for Dynamic Systems*. Boston: Kluwer Academic Publishers, 1999.
- M. G. El-Ghatwary, S. X. Ding, and Z. Gao. Robust fault detection for uncertain takagi-sugeno fuzzy systems with parametric uncertainty and process disturbances. In *Proceedings of IFAC Symp. SAFEPROCESS*, pages 787–792, Beijing, 2006.
- P. M. Frank and X. Ding. Survey of robust residual generation and evaluation methods in observer-based fault detection systems. *Journal of Process Control*, 7(6):403–424, December 1997. ISSN 0959-1524.
- M. Hou and R. J. Patton. An LMI approach to H_-/H_∞ fault detection observers. In *Proc. of UKACC Int. Conf. on Control '96*, volume 1, pages 305–310, 1996.
- H.Szu and R.Hartley. Fast simulated annealing. *Physics Letters A*, 122(3,4), 1987.
- Imad M. Jaimoukha, Zhenhai Li, and Vasilios Papakos. A matrix factorization solution to the H_-/H_∞ fault detection problem. *Automatica*, 42:1907–1912, 2006.
- S. Kirkpatrick, C. D. Gelatt, and M. P. Vecchi. Optimization by simulated annealing. *Science*, 220(4598): 671–680, 1983.
- G.P. Liu and R. J. Patton. *Eigenstructure Assignment for Control system Design*. Wiley, 1998.
- Ron J. Patton and Jie Chen. On eigenstructure assignment for robust fault diagnosis. *International Journal of Robust and Nonlinear Control*, 10(14):1193–1208, December 2000. ISSN 1049-8923.
- P.Sibani P.Salamon and R. Frost. *Facts, Conjectures, and Improvements for Simulated Annealing*. S.I.A.M, 2002.
- G. Roppenecker and J. Oreilly. Parametric output-feedback controller-design. *Automatica*, 25(2):259–265, March 1989. ISSN 0005-1098.
- N. Metropolis A.W. Rosenbluth M.N. Rosenbluth A.H. Teller and E. Teller. Equations of state calculations by fast computing machines. *Journal of Chemical Physics*, 21(6):1087–1092, 1953.
- T.W.Manikas and J.T.Cain. Genetic algorithms vs. simulated annealing: A comparison of approaches for solving the circuit partitioning problemg. Technical report, Department of Electrical Engineering, The University of Pittsburgh, Pittsburgh, 1996.
- H. B. Wang, J. L. Wang, and J. Lam. Robust fault detection observer design: Iterative LMI approaches. *Journal of Dynamic Systems Measurement and Control-Transactions of the Asme*, 129(1):77–82, January 2007a. ISSN 0022-0434.
- Jian. Liang. Wang. Guang. Hong. Yang, and Jian. Liu. An LMI approach to h_- index and mixed h_-/h_∞ fault detection observer design. *Automatica*, 43(9):1656–1665, September 2007b. ISSN 0005-1098.